Journal of Radiation Research, Vol. 58, No. 2, 2017, pp. 195–200
doi: 10.1093/jrr/rrw106
Advance Access Publication: 3 November 2016

Alpha-particle fluence in radiobiological experiments

Dragoslav Nikezic[1,2] and Kwan Ngok Yu[1,3*]

[1]Department of Physics and Materials Science, City University of Hong Kong, Kowloon Tong, Hong Kong
[2]Faculty of Science, University of Kragujevac, Kragujevac, Serbia
[3]State Key Laboratory in Marine Pollution, City University of Hong Kong, Kowloon Tong, Hong Kong
*Corresponding author. Department of Physics and Materials Science, City University of Hong Kong, Tat Chee Avenue, Kowloon Tong, Hong Kong. Tel: +852-3442-7812; Fax: +852-3442-0538; Email: peter.yu@cityu.edu.hk
Received August 5, 2016; Accepted October 3, 2016

ABSTRACT

Two methods were proposed for determining alpha-particle fluence for radiobiological experiments. The first involved calculating the probabilities of hitting the target for alpha particles emitted from a source through Monte Carlo simulations, which when multiplied by the activity of the source gave the fluence at the target. The second relied on the number of chemically etched alpha-particle tracks developed on a solid-state nuclear track detector (SSNTD) that was irradiated by an alpha-particle source. The etching efficiencies (defined as percentages of latent tracks created by alpha particles from the source that could develop to become visible tracks upon chemical etching) were computed through Monte Carlo simulations, which when multiplied by the experimentally counted number of visible tracks would also give the fluence at the target. We studied alpha particles with an energy of 5.486 MeV emitted from an ^{241}Am source, and considered the alpha-particle tracks developed on polyallyldiglycol carbonate film, which is a common SSNTD. Our results showed that the etching efficiencies were equal to one for source–film distances of from 0.6 to 3.5 cm for a circular film of radius of 1 cm, and for source–film distances of from 1 to 3 cm for circular film of radius of 2 cm. For circular film with a radius of 3 cm, the etching efficiencies never reached 1. On the other hand, the hit probability decreased monotonically with increase in the source–target distance, and fell to zero when the source–target distance was larger than the particle range in air.

KEYWORDS: alpha particle, fluence, solid-sate nuclear track detector, SSNTD, PADC, CR-39

INTRODUCTION

The radiobiological effects of alpha particles have attracted a lot of research interest due to their much larger linear energy transfer (LET) values than those of the more extensively studied X-ray or γ-ray photons, and due to the fact that they can be conveniently controlled to hit only a portion of the cells in a population, thus facilitating studies on the radiation-induced bystander effect (RIBE) [1–9] and the rescue effect [10–13] in a cell co-culture. It has been a common practice to characterize the extent of alpha-particle irradiation by the dose absorbed by a cell layer. In general, the alpha-particle dose rate (dD/dt) (in cGy/s) absorbed by the cell layer has been calculated using equations similar to that used by Inkret *et al.* [14]:

$$\frac{dD}{dt} = K \times \int S(E)\phi(E)dE, \quad (1)$$

where

E = alpha-particle energy (in MeV);
$\phi(E)dE$ = alpha-particle flux [or fluence rate $(d\Phi/dt)dE$] in the energy range from E to $E + dE$ (in $cm^{-2}\,s^{-1}$);
$S(E)$ = mass stopping power for alpha particle with energy E in tissue (in MeV g^{-1} cm^2);
K = the conversion to dose factor, i.e. 1.6022×10^{-8} [in cGy/(MeV g^{-1} cm^2)].

Equation (1) was valid for generic alpha-particle sources with an energy spectrum so that the flux $\phi(E)$ and the stopping power in tissue $S(E)$ were functions of the alpha-particle energy E. In reality, monoenergetic or pseudo-monoenergetic alpha-particle sources are commonly used for radiobiological experiments. One of the most

popular alpha-particle sources is the ^{241}Am source, which emits alpha particles with energies of 5.486, 5.443 and 5.388 MeV, with branching ratios of 85, 13 and 2%, respectively. Due to the similar alpha-particle energies, the ^{241}Am source can be treated as a pseudo-monoenergetic alpha-particle source. For a monoenergetic alpha-particle source, Eq. (1) can be simplified as:

$$\frac{dD}{dt} = K \times S \times \phi, \tag{2}$$

where

ϕ = alpha-particle flux for the alpha particles (in cm^{-2} s^{-1}); and
S = mass stopping power for the alpha particles in tissue (in MeV g^{-1} cm^2).

The dose D, which has been commonly used to characterize the extent of alpha-particle irradiation is then given by:

$$D = \int \left(\frac{dD}{dt}\right) dt = K \times S \times \phi \times \Delta t = K \times S \times \Phi, \tag{3}$$

where Δt (in s) is the total time of irradiation and Φ (in cm^{-2}) = $\phi \times \Delta t$ is the fluence.

To evaluate the dose D, the alpha-particle flux ϕ or fluence Φ need to be determined, either theoretically or experimentally. Theoretical determination relies on the activity of the source provided by the manufacturer (usually given as the total activity present in the source), while experimental determination is usually achieved through counting the number of chemically etched alpha-particle tracks developed on the solid-state nuclear track detector (SSNTD) having been irradiated by the alpha-particle source. When an alpha particle or a heavy ion hit an SSNTD, a damaged volume (called the latent track) is formed along the trajectory of the particle. When the SSNTD with latent tracks is immersed in an etching solution ('etchant'), the etching rate along the latent track (called the track etch velocity V_t) is larger than the etching rate of the undamaged SSNTD material (called the bulk etch velocity V_b) [15]. Development of the track would depend on the V function ($V = V_t/V_b$). Under appropriate conditions, including a sufficiently large incidence angle of the particle with respect to the SSNTD surface (larger than the 'critical angle'), and a sufficiently large total removed layer upon chemical etching, the latent tracks can be enlarged to become visible under the optical microscope [15].

However, both of these methods have inherent difficulties. For example, most alpha-particle sources used for radiobiological experiments have a 2π geometry, i.e. the alpha particles are not collimated and do not travel in the same direction. For theoretical determination of the fluence, at least 50% of the alpha particles would be lost because of the 2π geometry. A further complication arises from the fact that the fraction of alpha particles reaching the target depends on the solid angle subtended by the target at the source, which would decrease as the distance between the source and the target (hereafter referred to as the source–target distance) increases. Furthermore, when the alpha particles are emitted in very oblique directions, they might not be able to reach the target because the distance needed to be traveled exceeds the ranges of the alpha particles. For experimental determination of the fluence, it is well established that the feasibility of revealing an alpha-particle track on the SSNTD through chemical etching strongly depends on the energy and the incidence angle of the alpha particle (with respect to the SSNTD surface) when it hits the SSNTD. When an alpha particle hits the SSNTD with a very small incidence angle, or with a very small energy after losing its energy through traveling a long distance in air, the corresponding latent track could not be etched to form a visible track [15]. All these factors would lead to deviations in the determined fluence from the true value, and would therefore introduce errors in the reported dose D.

Besides the dose absorbed by the cell layer, which characterizes the level of alpha-particle irradiation, in determining the targeted effect (i.e. the effect of direct irradiation) or of the non-targeted effects [such as radiation-induced bystander effect (RIBE) or rescue effect] it is important to obtain an accurate average number (n) of hits on a single cell in the culture dish. For example, to prepare a homogeneous population of irradiated cells, i.e. not mixed with unirradiated cells, it is important to make sure that every single cell in the population was very likely hit by at least one alpha particle, since the presence of unirradiated cells would introduce the rescue effect [11, 12] and would affect and complicate the studied RIBE. The probability that each cell would be hit by at least one alpha particle is given by the Poisson statistics as $[1 - \exp(-n)]$. The average number n of alpha-particle hits on a cell with an area A is given by:

$$n = A \times \Phi, \tag{4}$$

which is also sometimes expressed as $n = (A \times D)/(K \times S)$. As such, accurate values of Φ or D would be very important in the design of experiments to study the targeted and non-targeted bystander effects of alpha particles.

The present work was devoted to determining the alpha-particle fluence for radiobiological experiments with the help of Monte Carlo simulations. For theoretical determinations, the probabilities of the target (cell layer of SSNTD) being hit by alpha particles emitted from the source (i.e. hit probabilities) were computed. We note that the hit probabilities were defined in the present work based on an isotropic (i.e. 4π) source, so that multiplying the hit probability by the activity (total activity present in the source) provided by the manufacturer would give the expected fluence at the target for specific source–target distances. For experimental determinations, an SSNTD was located on the inner bottom of the Petri dish in which the cells were to be cultured, which was set at a chosen distance from the alpha-particle source. After irradiation by the alpha-particle source for a specified time, the SSNTD was chemically etched, and the developed alpha-particle tracks were counted under an optical microscope. In addition, the percentages of the latent tracks created by alpha particles from the source during irradiation that could develop to become visible under the optical microscope upon chemical etching (hereafter referred to as the 'etching efficiencies') were theoretically evaluated. These data were employed together to give the true number of alpha-particle hits on the SSNTD, thus giving the fluence for chosen source–target distances.

METHODS

In the present work, for illustration purposes we studied alpha particles emitted from an ^{241}Am source with a circular active area with a diameter of 5 mm. ^{241}Am sources are commonly used in radiobiological studies [12, 13, 16–22]. For simplicity, in all computations in the present work, we considered that all the alpha particles were emitted with the energy of 5.486 MeV. Considering all three alpha-particle energies together with their branching ratios, or considering other alpha-particle sources would not qualitatively change the conclusions of the present work. We also studied the alpha-particle tracks developed on polyallyldiglycol carbonate (PADC) film using the V function from Brun *et al.* [23] with a bulk etch rate V_b of 1.37 μm/h [15]. PADC film (commercially available as CR-39 detector) is commonly employed to provide information on the fluence of alpha particles or heavy ions. The value of V_b was in fact not crucial because all the final results would depend on the total removed layer (i.e. V_b × etching period) [15]. The current results could still be valid for PADC films with different V_b values, with the only change needed being the etching time to keep the total removed layer the same. The methodology developed in the present work could be extended to studies using other SSNTDs, such as cellulose nitrate film (commercially available as LR 115 detector) or polycarbonate film (commercially available as Makrofol detector).

For illustration purposes, we only performed our calculation for a Petri dish that had a radius of 3 cm. When determining the etching efficiencies for PADC films, each PADC film was assumed to have been placed on the inner bottom of a Petri dish used to culture the cells to be irradiated. The PADC films were assumed to be circular, with radii of 1, 2 and 3 cm. It was known that PADC film is brittle, and that it is difficult to prepare a circular film; however, the results in the present work could still be used even when a square film was irradiated. A circle with the desired radius can be drawn on the square film and only the tracks within the circle counted. The ^{241}Am alpha-particle source was located above the Petri dish at various source–target distances.

When the target (cell layer or PADC film) was irradiated with the ^{241}Am source, there were a number of possible fates for the alpha particles, as shown in Fig. 1. For Case 1, the alpha particle was emitted in such a direction that it could not hit the target. For Case 2, the alpha particle was emitted towards the target, but the emission was in such a direction that the alpha particle could not reach the target because it was absorbed by the air due to the finite range of the alpha particle. For Case 3, the alpha particle hit the target, and could be absorbed within the target or could penetrate through the target. In Case 3, if the target was a PADC film and if the incidence angle of the alpha particle was larger than a critical angle [15], the latent track would become visible after chemical etching for an appropriate period, and could be counted under an optical microscope.

The simulations in the present work consisted of the following steps:

(i) Sampling of the starting point of an alpha particle in the source. The source was assumed to be thin, such that there was no self-absorption in the source.

(ii) Sampling of the initial direction of the alpha-particle motion according to the formula for random direction, which was determined by two angles, θ_{RN} and φ_{RN}, i.e.

$$\cos(\theta_{RN}) = 2 \times RN_1 - 1 \text{ and } \varphi_{RN} = 2\pi \times RN_2,$$

where RN_i were random numbers.

(iii) Determination of whether the alpha particle hit the target. If not, the simulation went back to step (1), i.e. to sample a new alpha particle. The counter for the number of simulations, where each simulation represented one emitted alpha particle, was increased by one.

(iv) If the alpha particle hit the PADC film, it was necessary to determine whether the latent track would be visible after chemical etching. To help with this decision, the computer programs TRACK_TEST [24] and TRACK_VISION [25] were applied. The program TRACK_TEST was originally developed for calculation of track parameters and graphical representation of a chemically etched track. For the

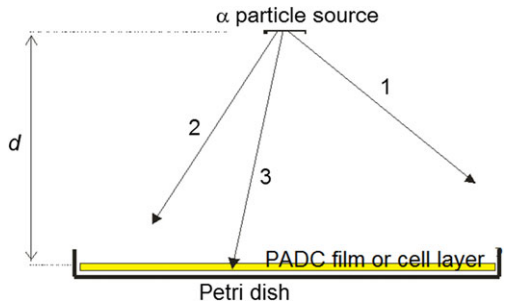

Fig. 1. Schematic diagram showing the irradiation of the target (cell layer or PADC film located on the inner bottom of the Petri dish) with the ^{241}Am source, with d as the vertical distance between the ^{241}Am source and the target. The three possible fates for the alpha particles (labeled as 1, 2 and 3) are explained in the text.

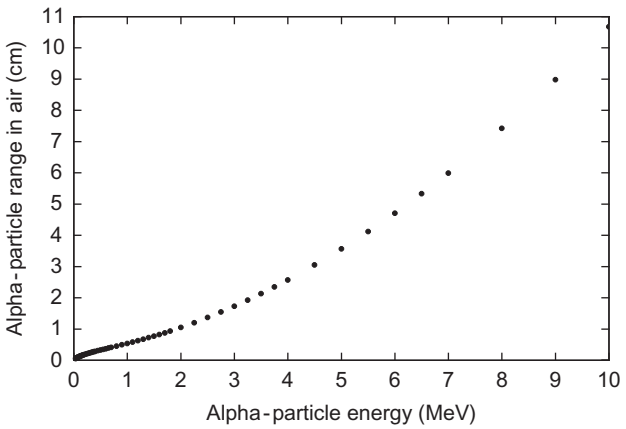

Fig. 2. Relationship between the alpha-particle range in air (cm) and the alpha-particle energy (MeV). The output was generated using the SRIM code [26].

purpose of simulation in this work, the graphical routines were disabled so that only the track parameters, namely, the lengths of the major axes and minor axes, as well as the track depth, were calculated for each alpha particle that hit the PADC film. We only considered those tracks with all three calculated parameters >1 μm, and those with at least a dark portion when viewed under an optical microscope as 'visible' tracks under the optical microscope [25]. If the track was considered visible, the counter for the number of visible tracks was increased by one.

When the alpha particles passed through the air, some of their energies were lost. The stopping power and range of alpha particles in various media were calculated using the SRIM program [26]. The ranges of alpha particles in (dry) air obtained using SRIM are presented in Fig. 2.

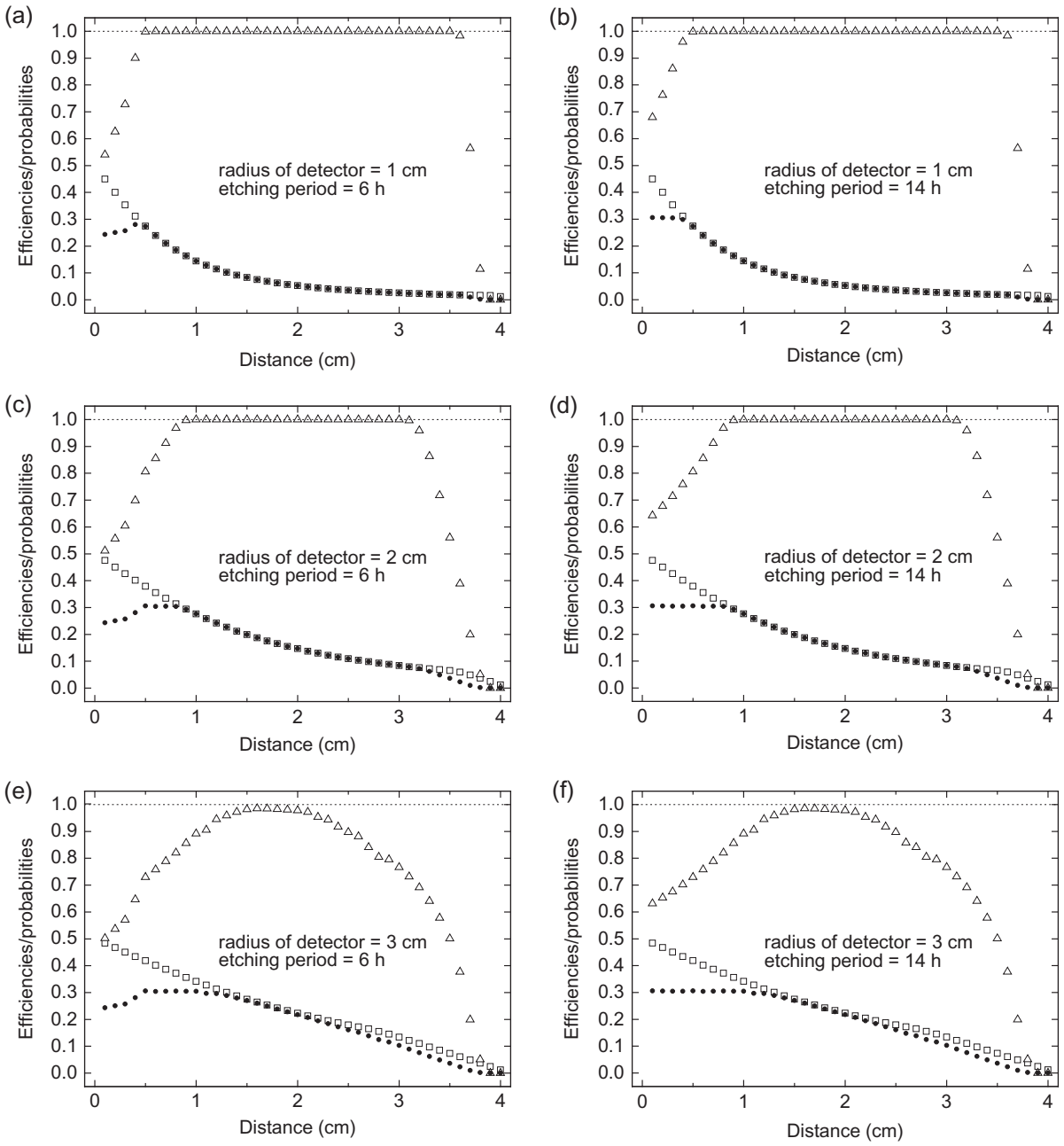

Fig. 3. Dependence of the etching efficiency, hit probability and overall detection efficiency for PADC film irradiated by alpha particles from an ^{241}Am radioactive source on source–film distance for film radii of 1 cm [(a) and (b)], 2 cm [(c) and (d)], and 3 cm [(e) and (f)], and for etching times of 6 h [(a), (c) and (e)] and 14 h [(b), (d) and (f)]. Open squares: hit probability; open triangles: etching efficiency; solid circles: overall detection efficiency; dotted line: etching efficiency = 1.

RESULTS AND DISCUSSION

Figure 3 shows the dependence of the etching efficiency, hit probability and overall detection efficiency for ADC film irradiated by alpha particles from an ^{241}Am radioactive source on the distance between the alpha-particle source and the PADC film (hereafter referred to as the source–film distance) for film radii of 1, 2 and 3 cm, and for etching times of 6 and 14 h. The overall detection efficiency was the product of the hit probability and the etching efficiency. Figure 3 shows that changing the etching period from 6 to 14 h did not significantly affect these probabilities and efficiencies.

The relationship between the etching efficiency and the source–film distance was complicated. For small source–film distances, namely, distances less than 0.6, 1 and 1.5 cm in the cases of films with radii of 1, 2 and 3 cm, respectively, a significant portion of the emitted alpha particles would hit the film with very small incidence angles, i.e. with very slanted incidence, and their latent tracks could not be etched to form visible tracks. This explained the reduction in both the etching efficiency and the overall detection efficiency at small distances. For large source–film distances, namely, distances larger than 3.5, 3 and 1.9 cm in the cases of films with radii of 1, 2 and 3 cm, respectively, a significant portion of the emitted alpha particles would hit the film after traveling a distance close to the particle range, and as a result the incidence energies of these alpha particles would be small, causing the etching efficiency to drop sharply. Consequently, the detection efficiency would also drop. For intermediate source–film distances, the incidence angles of alpha particles were large, which led to etching efficiencies close to or equal to 1. As such, most latent tracks became visible after the chemical etching. The etching efficiencies were equal to one for source–film distances from 0.6 to 3.5 cm for film with a radius of 1 cm, and for source–film distances from 1 to 3 cm for film with a radius of 2 cm. We note that for film with a radius of 3 cm, the etching efficiencies never reached 1, but were >0.98 for source–film distances from 1.5 to 1.9 cm, with the mean ± S.D. = 0.983 ± 0.002. To apply these results in the experimental determination of the alpha-particle fluence, one would need to choose film with a radius that matched that of the Petri dish to be used for culturing cells for the alpha-particle irradiation (the results were given for films with radii of 1, 2 or 3 cm in the present work), and one would also need to choose a source–film distance that matched the distance between the source and the cell layer during the alpha-particle irradiation. The number of visible etched tracks developed on the PADC film (after 6 to 14 h of etching) was then counted under the optical microscope, and then multiplied by the corresponding etching efficiency to give the alpha-particle fluence.

In contrast to the complicated relationship between the etching efficiency and the source–film distance, the behavior of the hit probability was much simpler. The hit probability decreased monotonically with increase in the source–target distance, and fell to zero when the source–target distance was larger than the particle range in air. When the source was very close to the target, e.g. when the distance was < 0.1 cm, the hit probabilities were ~50% in all cases (for various target radii and etching periods), which was expected because emission was isotropic (4π) as defined above, and half of the alpha particles were emitted towards the target, while the other half were moving in the opposite direction. As the source–target distance increased, the number of alpha particles that hit the target decreased (due to the decreasing solid angle subtended by the target at the source).

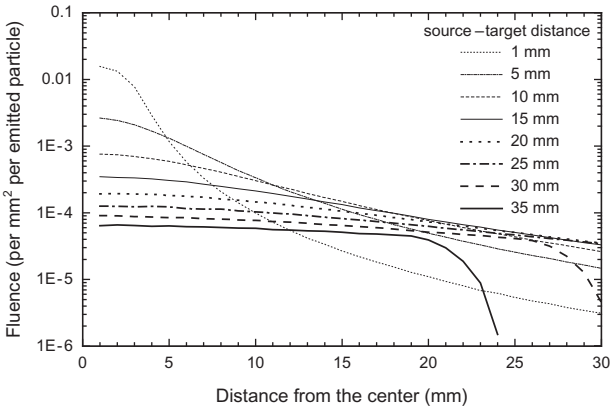

Fig. 4. Relationship between fluence (mm^{-2} per emitted alpha particle) and the radial distance from the center of the target, calculated for various source–target distances.

The results for the hit probabilities might lead to a temptation to use very small source–target distances to maximize the hit probability. However, small source–target distances would lead to inhomogeneous fluence. Figure 4 shows the relationship between the alpha-particle fluence (mm^{-2} per emitted alpha particle) and the radial distance from the center of the target, calculated for various source–target distances. One can see that for small source–target distances, e.g. 1 mm, effectively only the central part of the target was irradiated. The fluence decreased sharply with distance from the center of the target. By moving the source away from the target, a larger part of the target became irradiated, but the fluence always decreased towards the rim of the target. This can be explained by the range of ~4.1 cm for an alpha particle with an energy of 5.486 MeV in air.

For clearer explanations, the inhomogeneity of the fluence was characterized by the ratio R = (fluence at 10 mm from the center of the target)/(fluence at 1 mm from the center of the target). The ratios were 0.00637, 0.128, 0.399, 0.610, 0.754, 0.824, 0.846 and 0.915 for source–target distances of 1, 5, 10, 15, 20, 25, 30 and 35 mm, respectively. Values of R much smaller than unity could lead to large differences in the average number n of alpha-particle hits on cells and thus in the doses received by cells located at various radial distances from the center. In some extreme cases, n would become very small, and the probability that each cell would be hit by at least one alpha particle, namely, $[1 - \exp(-n)]$, would become large. Under such circumstances, some cells located further away from the center of the field of irradiation might not be hit by any alpha particles. This would be an undesirable situation because the irradiated population of cells would be inhomogeneous and would consist of both irradiated and non-irradiated cells—and the presence of unirradiated cells would introduce the rescue effect and would affect and

complicate the studied RIBE. From the present results, it appears that a source–target distance of 35 mm and a Petri dish with a radius of ≤10 mm were needed to achieve good homogeneity, although source–target distances of 25 and 30 mm were also acceptable. However, it should also be noted that the fluence also decreased with increasing source–target distances due to the reduced hit probabilities. To overcome this, it would be necessary to use either a strong alpha-particle source or a long irradiation time, but the latter would induce extra stress in the cells, which might also complicate the biological effects.

ACKNOWLEDGEMENTS

We acknowledge the support of the Neutron computer cluster of the Department of Physics and Materials science, City University of Hong Kong, for the computational work involved in this paper.

CONFLICT OF INTEREST

The authors declare that there are no conflicts of interest.

REFERENCES

1. Nagasawa H, Little JB. Induction of sister chromatid exchanges by extremely low doses of alpha-particles. *Cancer Res* 1992;52:6394–6.
2. Deshpande A, Goodwin EH, Bailey SM, et al. Alpha-particle–induced sister chromatid exchange in normal human lung fibroblasts: evidence for an extranuclear target. *Radiat Res* 1996;145:260–7.
3. Prise KM, Belyakov OV, Folkard M, et al. Studies of bystander effects in human fibroblasts using a charged particle microbeam. *Int J Radiat Biol* 1998;74:793–8.
4. Zhou H, Randers-Pehrson G, Waldren CA, et al. Induction of a bystander mutagenic effect of alpha particles in mammalian cells. *Proc Natl Acad Sci USA* 2000;97:2099–104.
5. Zhou H, Suzuki M, Randers-Pehrson G, et al. Radiation risk to low fluences of alpha particles may be greater than we thought. *Proc Natl Acad Sci U S A* 2001;98:14410–5.
6. Azzam EI, De Toledo SM, Spitz DR, et al. Oxidative metabolism modulates signal transduction and micronucleus formation in bystander cells from alpha-particle–irradiated normal human fibroblast cultures. *Cancer Res* 2002;62:5436–42.
7. Shao C, Stewart V, Folkard M, et al. Nitric oxide–mediated signaling in the bystander response of individually targeted glioma cells. *Cancer Res* 2003;63:8437–42.
8. Mitchell SA, Randers-Pehrson G, Brenner DJ, et al. The bystander response in C3H 10T1/2 cells: the influence of cell-to-cell contact. *Radiat Res* 2004;161:397–401.
9. Zhou H, Ivanov VN, Lien YC, et al. Mitochondrial function and nuclear factor-kappaB–mediated signaling in radiation-induced bystander effects. *Cancer Res* 2008;68:2233–40.
10. Chen S, Zhao Y, Han W, et al. Rescue effects in radiobiology: unirradiated bystander cells assist irradiated cells through intercellular signal feedback. *Mutat Res* 2011;706:59–64.
11. Lam RKK, Fung YK, Han W, et al. Rescue effects: irradiated cells helped by unirradiated bystander cells. *Int J Mol Sci* 2015;16:2591–609.
12. Lam RKK, Han W, Yu KN. Unirradiated cells rescue cells exposed to ionizing radiation: activation of NF-κB pathway in irradiated cells. *Mutat Res* 2015;782:23–33.
13. Lam RKK, Fung YK, Han W, et al. Modulation of NF-κB in rescued irradiated cells. *Radiat Prot Dosim* 2015;167:37–43.
14. Inkret WC, Eisen Y, Harvey WF, et al. Radiobiology of alpha particles. I. Exposure system and dosimetry. *Radiat Res* 1990;123:304–10.
15. Nikezic D, Yu KN. Formation and growth of tracks in nuclear track materials. *Mater Sci Eng R* 2004;46:51–123.
16. Wang R, Coderre JA. A bystander effect in alpha-particle irradiations of human prostate tumor cells. *Radiat Res* 2005;164:711–22.
17. Esposito G, Antonelli F, Belli M, et al. An alpha-particle irradiator for radiobiological research and its implementation for bystander effect studies. *Radiat Res* 2009;172:632–42.
18. Chen S, Zhao Y, Zhao G, et al. Up-regulation of ROS by mitochondria-dependent bystander signaling contributes to genotoxicity of bystander effects. *Mutat Res* 2009;666:68–73.
19. Han W, Chen S, Yu KN, et al. Nitric oxide mediated DNA double strand breaks induced in proliferating bystander cells after alpha-particle irradiation. *Mutat Res* 2010;684:81–9.
20. Han W, Wu L, Chen S, et al. Exogenous carbon monoxide protects the bystander Chinese hamster ovary cells in mixed coculture system after alpha-particle irradiation. *Carcinogenesis* 2010;31:275–80.
21. Han W, Yu KN, Wu LJ, et al. Mechanism of protection of bystander cells by exogenous carbon monoxide: impaired response to damage signal of radiation-induced bystander effect. *Mutat Res* 2011;709–10:1–6.
22. Yin X, Tian W, Wang L, et al. Radiation quality–dependence of bystander effect in unirradiated fibroblasts is associated with TGF-β1-Smad2 pathway and miR-21 in irradiated keratinocytes. *Sci Rep* 2015;5:11373.
23. Brun C, Fromm M, Jouffroy M, et al. Intercomparative study of the detection characteristics of the CR-39 SSNTD for light ions: present status of the Besancon–Dresden approaches. *Radiat Meas* 1999;31:89–98.
24. Nikezic D, Yu KN. Computer program TRACK_TEST for calculating parameters and plotting profiles for etch pits in nuclear track materials. *Comput Phys Commun* 2006;174:160–5.
25. Nikezic D, Yu KN. Computer program TRACK_VISION for simulating optical appearance of etched tracks in CR-39 nuclear track detectors. *Comput Phys Commun* 2008;178:591–5.
26. Ziegler JF, Ziegler MD, Biersack JP. SRIM – the stopping and range of ions in matter. *Nucl Instrum Meth B* 2010;268:1818–23.